Electronic Supplementary Information (ESI):

Electrochemical tuning of olivine-type lithium transition-metal phosphates as efficient water oxidation catalysts

Yayuan Liu, [a] Haotian Wang, [b] Dingchang Lin, [a] Chong Liu, [a] Po-Chun Hsu, [a] Wei Liu, [a] Wei Chen, [a] and Yi Cui* [a c]

[a] Department of Materials Science and Engineering, Stanford University, Stanford, CA 94305, USA

[b] Department of Applied Physics, Stanford University, Stanford, CA 94305, USA

[c] Stanford Institute for Materials and Energy Sciences, SLAC National Accelerator Laboratory, 2575 Sand Hill Road, Menlo Park, California 94025, USA

Experimental Details

Synthesis of submicrometer-sized $LiCoPO_4$ particles (LCoP): LCoP particles were synthesized using sol-gel method. In a typical synthesis, 0.01 mol of $LiNO_3$, 0.01 mol of $Co(CH_3COO)_2$, 0.01 mol of $NH_4H_2PO_4$ and 0.03 mol of citric acid were dissolved in 10 ml distilled water at room temperature. The pH of the resulting solution was maintained below 4 using HNO_3. Subsequently, the solution was heated at 80 ^oC in a water bath under constant stirring to obtain a viscous gel. The as-prepared gel was dried overnight at 120 °C, grinded and then calcined in air at 700 ^oC for 5 hrs to obtain the final purple-colored LCoP powder.

Synthesis of $Co_3(PO_4)_2$ particles: $Co_3(PO_4)_2$ particles were synthesized following the same procedure as LCoP by using 0.03 mol of $Co(CH_3COO)_2$, 0.02 mol of $NH_4H_2PO_4$ and 0.06 mol of citric acid as the precursor.

Synthesis of $LiMPO_4$/reduced graphene oxide composite (LMP/rGO): LMP/rGO composites were synthesized based on a previously reported two-step approach. Firstly, graphene oxide (GO, Graphene Supermarket, 5 g/L) was transferred from aqueous suspension to dimethylformamide (DMF) by centrifuging and the final concentration of the DMF suspension was ~0.2 mg/ml. In the first step of synthesis, 5 ml of GO DMF suspension was first heated to 80 °C in a 20 ml vial with magnetic stirring. Subsequently, 0.5 ml of 0.2 M aqueous solution of metal salt was quickly injected in (0.5 ml $Co(Ac)_2$ for LCoP/rGO; 0.4 ml $Co(Ac)_2$ and 0.1ml $Fe(NO_3)_3$ for LCoFeP/rGO; 0.4 ml $Mn(Ac)_2$ and 0.1ml $Fe(NO_3)_3$ for LMnFeP/rGO; 0.4 ml $Ni(Ac)_2$ and 0.1ml $Fe(NO_3)_3$ for LNiFeP/rGO; 0.2 ml $Co(Ac)_2$, 0.2 ml $Ni(Ac)_2$ and 0.1ml $Fe(NO_3)_3$ for LCoNiFeP/rGO). The reaction was kept at 80 °C under vigorous stirring for 1 hr and the reaction product was collected by centrifuge and redispersed in 10 ml DMF. In the second step of synthesis, 0.1 ml of 1M LiOH aqueous solution, 0.1 ml of 1M H_3PO4 and 0.5

ml of 0.5 M ascorbic acid DMF solution were added to the DMF suspension of the first-step reaction product to afford a homogeneous mixture. The mixture was then sealed in a 40 ml Teflon lined stainless steel autoclave and heated at 180 °C overnight. Then resulting product was washed with distilled water for 6 times and redispersed in 5 ml ethanol.

Electrochemical tuning of LCoP and LMP/rGO: LCoP particles along with 10 wt% Nafion® 117 solution (Sigma-Aldrich) and 20 wt% conducting carbon black were dispersed in ethanol by at least 30 min sonication to afford a homogeneous ink solution with a final catalyst concentration of 5 mg/ml. 200 µl of the abovementioned ink solution was loaded onto a 1 cm × 2 cm carbon fiber paper (Fuel Cell Store) to achieve a loading of 0.5 mg/cm^2. The concentration of the LMP/rGO composite in ethanol was determined by weighing the dried product of a certain amount of the dispersion after solvent evaporation. 10 wt% Nafion® 117 solution was added into the dispersion and sonicated for at least 30 min to form a homogeneous ink, which was subsequently loaded onto a 1 cm × 2 cm carbon fiber paper to achieve a final catalyst loading of 0.5 mg/cm^2. Afterwards, the carbon fiber paper electrodes were thoroughly dried and put into pouch cells as the cathode, which were assembled in argon-filled glove box free from oxygen and water. Li metal was used as the anode, 1 M $LiPF_6$ in 1:1 wt/wt ethylene carbonate/diethyl carbonate (BASF) was used as the electrolyte and polypropylene-based Celgard 2321 was used as the separator. The delithiation process was carried out by charging the samples to different potentials versus Li^+/Li with a constant current of 0.025 mA/cm^2. After delithiation, the samples were taken out and rinsed with ethanol.

Materials characterizations: FEI XL30 Sirion Scanning electron microscope was used to characterize the morphology of the samples. Powder X-ray diffraction (XRD) patterns were recorded on a PANalytical X'Pert instrument. Inductively coupled plasma-mass spectroscopy

(ICP-MS) was carried out using Thermo Scientific XSERIES 2. Thermogravimetric analyses (TGA) were performed on a TG 449 F3 Jupiter® Thermo-Microbalance in Argon atmosphere at 600 ^{o}C for 2 hrs with a heating rate of 10 ^{o}C/min. Raman Spectroscopy was carried out using WITEC Raman spectrometer (531-nm excitation laser, cutoff around 175 cm^{-1}) and XPS analysis was done on a SSI SProbe XPS spectrometer with Al(Ka) source.

Electrochemical characterizations: All the electrochemical studies were carried out using a Biologic VMP3 multichannel system. A typical three-electrode set-up was employed with a saturated calomel electrode (SCE) as reference electrode and a platinum wire as counter electrode. E(RHE) = E(SCE)+ 0.999 V in 0.1 M KOH and E(RHE) = E(SCE)+ 1.058 V in 1 M KOH (calibrated in H_2-saturated electrolyte with respect to an *in situ* RHE). Multiple cyclic voltammetry (CV) scans were performed until stable before the linear sweep voltammetry (LSV) curves were collected at a scan rate of 5 mv/s. And the LSV data was iR corrected. Chronopotentiometry was carried out under a constant current density of 10 mA/cm^2.

The electrochemical double-layer capacitance (EDLC) of the samples was measured by performing CV scans at various scan rates (30 mv/s, 20 mv/s, 10 mv/s, 5 mv/s and 2 mv/s) within the potential window where there is a non-Faradic current response (0.2 V – 0.3 V vs. SCE). The average current density at 0.25 V was plotted against scan rate and the slope of the linear fit curve is the EDLC.

Supplementary Figures

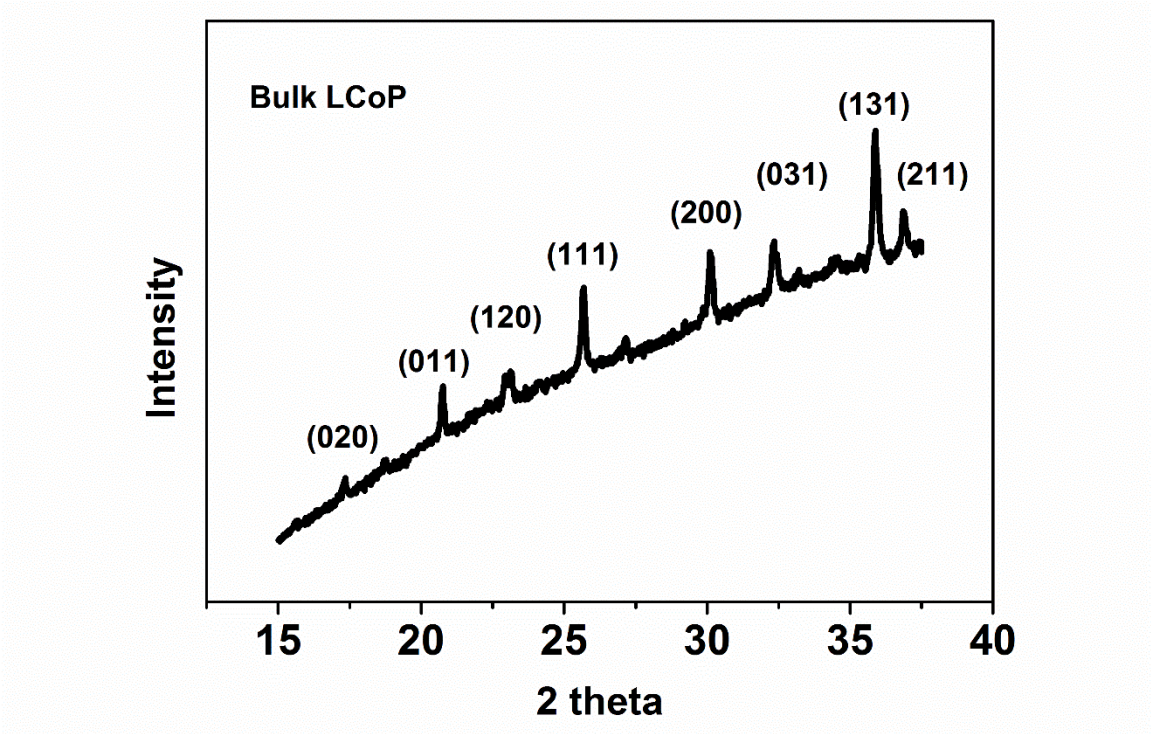

Fig. S1 XRD spectrum of submicron LCoP particles (JCPDS card No. 32- 0552).

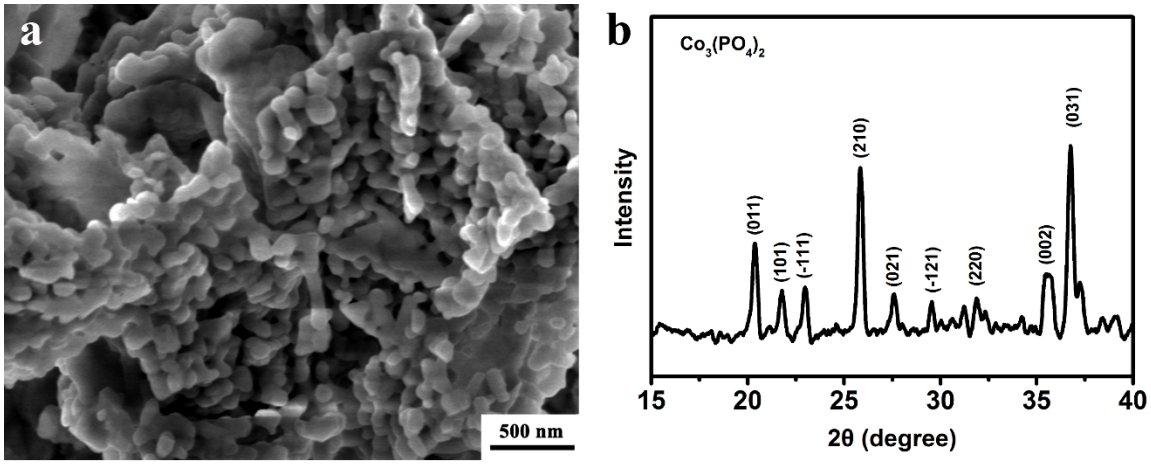

Fig. S2 (a) SEM image and (b) XRD spectrum of $Co_3(PO_4)_2$ particles (JCPDS card No. 13-0503).

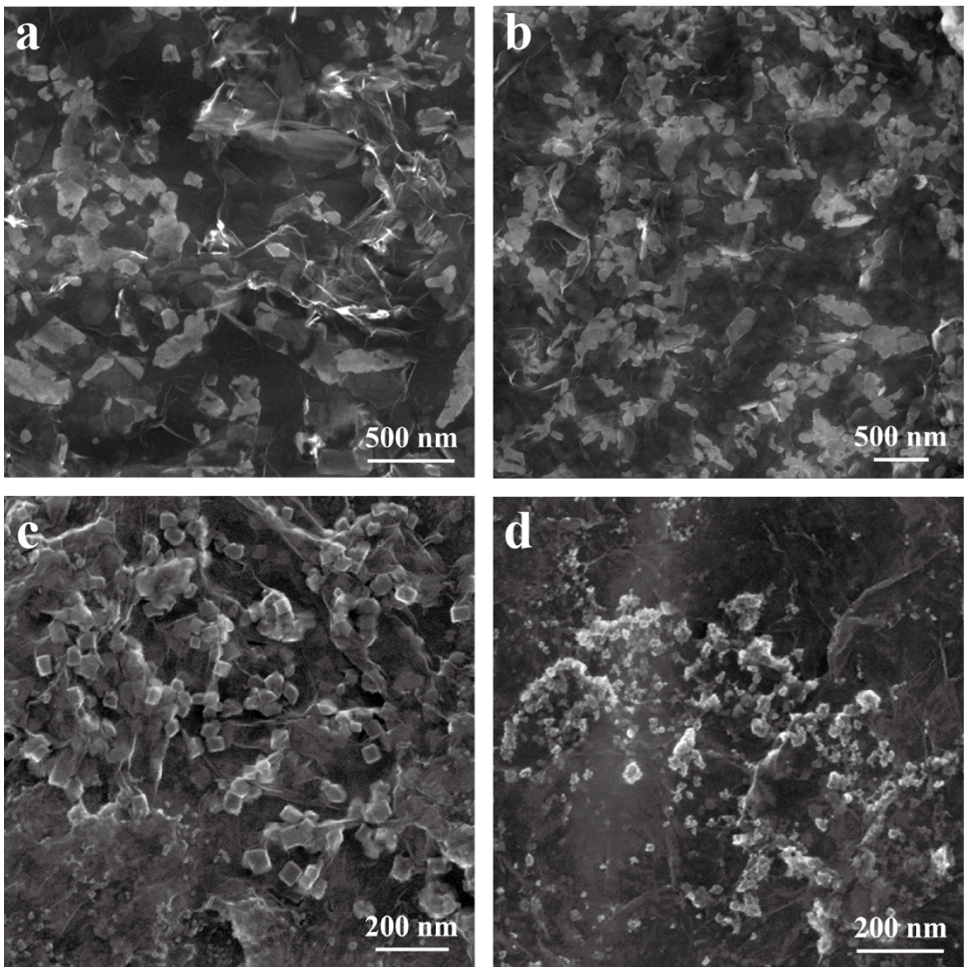

Fig. S3 SEM images of (a) LCoP/rGO, (b) LCoFeP/rGO, (c) LMnFeP/rGO and (d) LCoNiFeP/rGO.

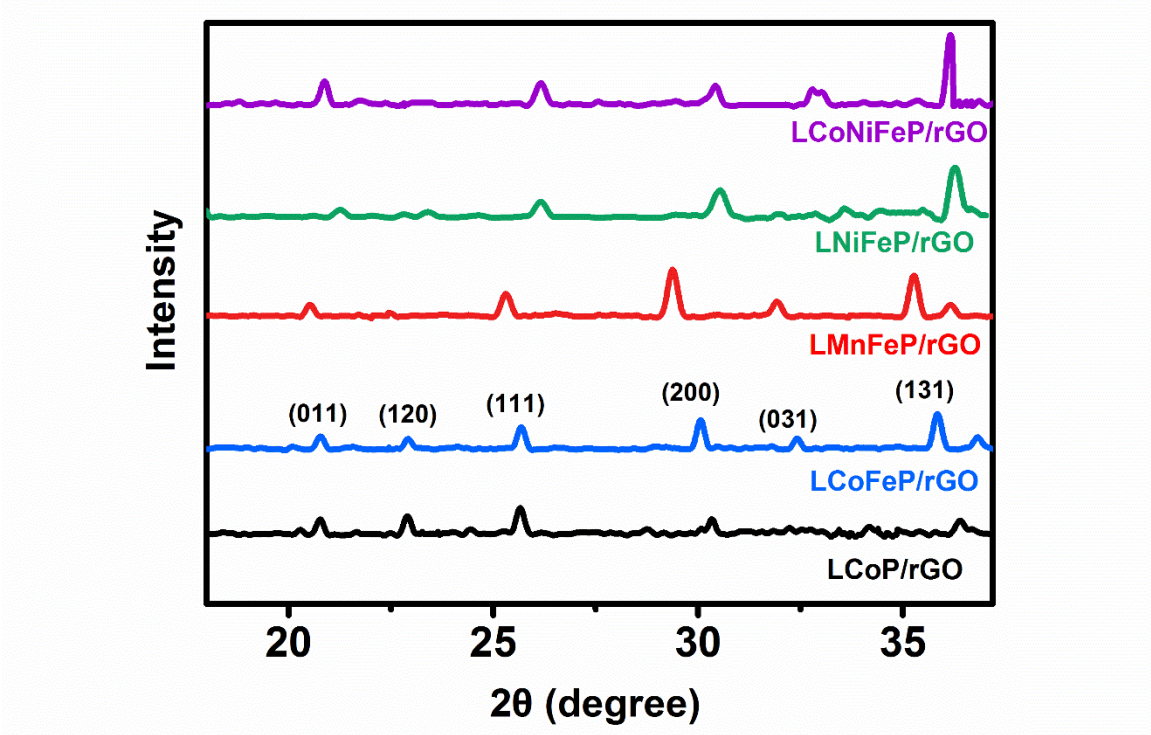

Fig. S4 XRD spectra of the $LiMPO_4$/rGO hybrid.

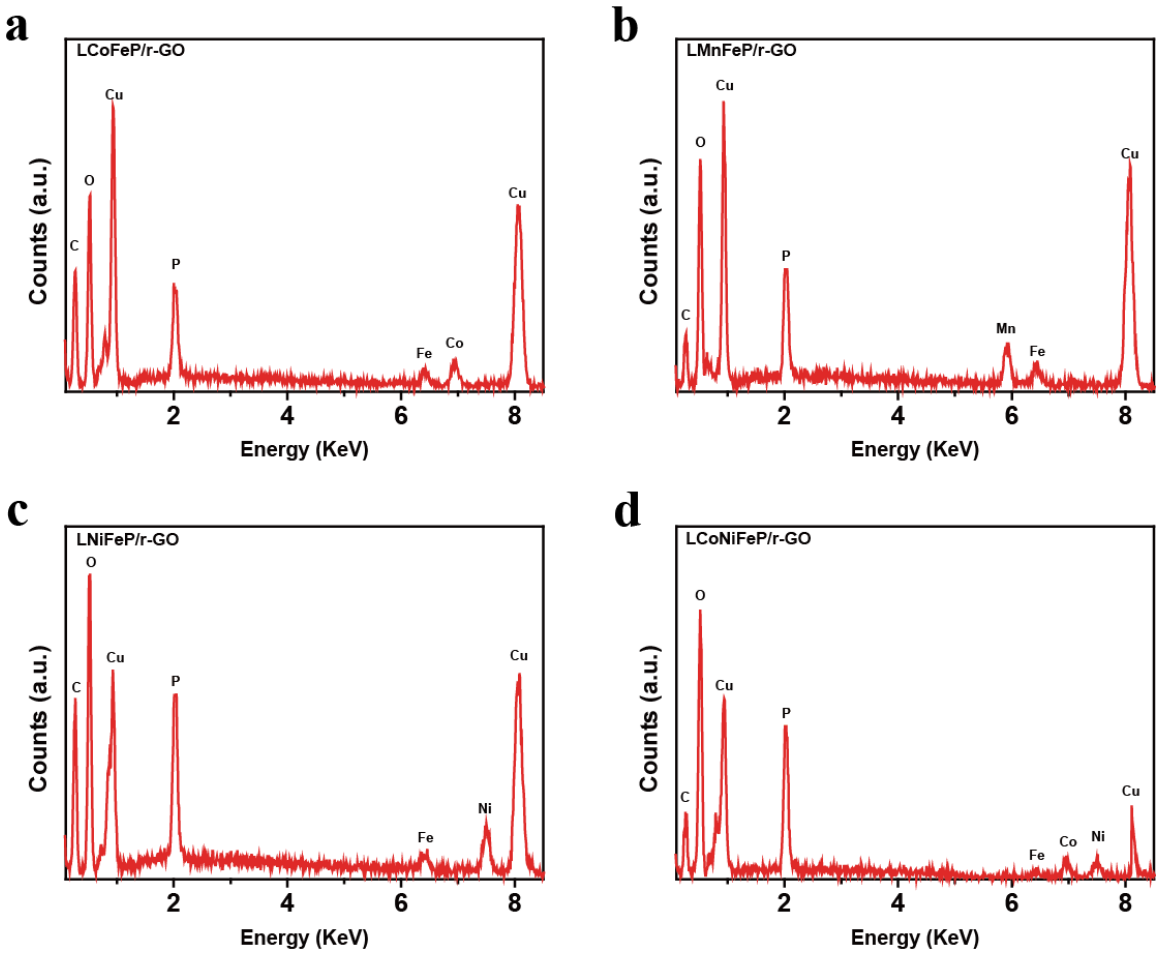

Fig. S5 EDX results of the LMP/rGO hybrids (Cu signal is due to the Cu substrate).

Table S1 Summary of the compositions of the LMP/rGO hybrids obtained by EDX.

Sample	Composition
LCoFeP/rGO	~$LiCo_{0.65}Fe_{0.35}PO_4$
LMnFeP/rGO	~$LiMn_{0.65}Fe_{0.35}PO_4$
LNiFeP/rGO	~$LiNi_{0.75}Fe_{0.25}PO_4$
LCoNiFeP/rGO	~$LiCo_{0.35}Ni_{0.50}Fe_{0.15}PO_4$

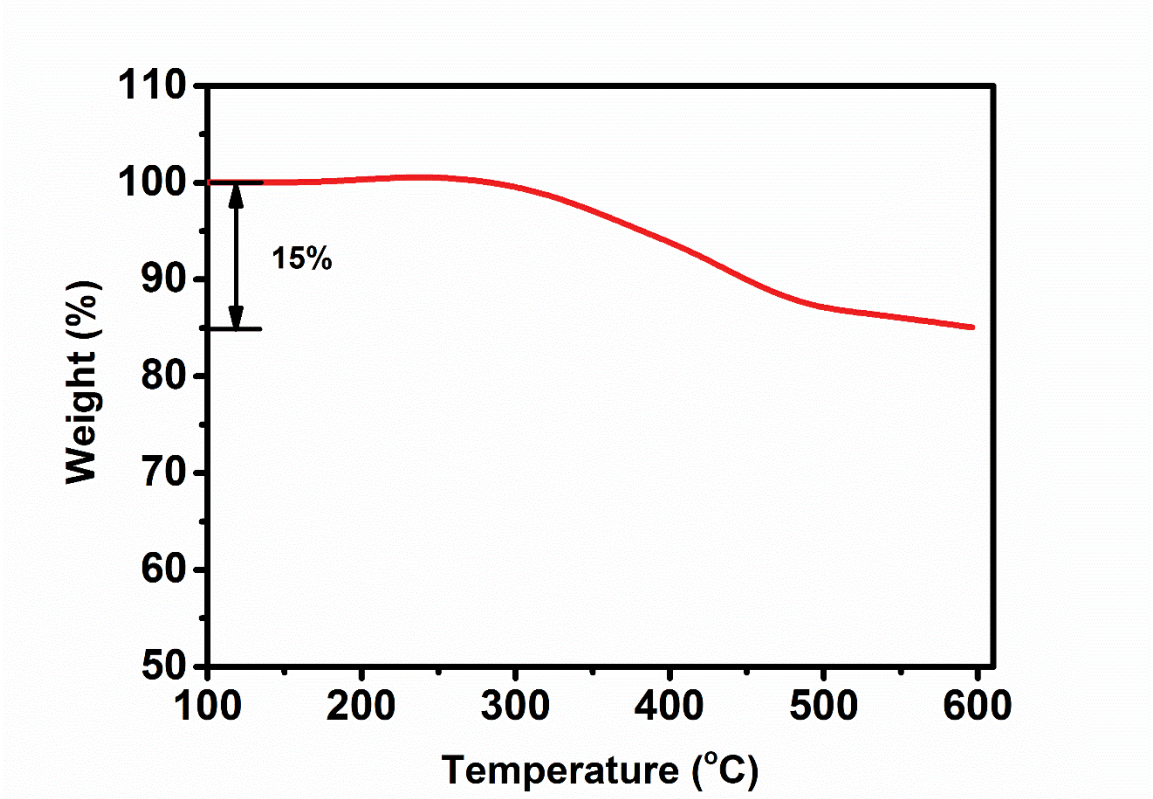

Fig. S6 TGA curve of the $LiCoPO_4$/rGO hybrid.

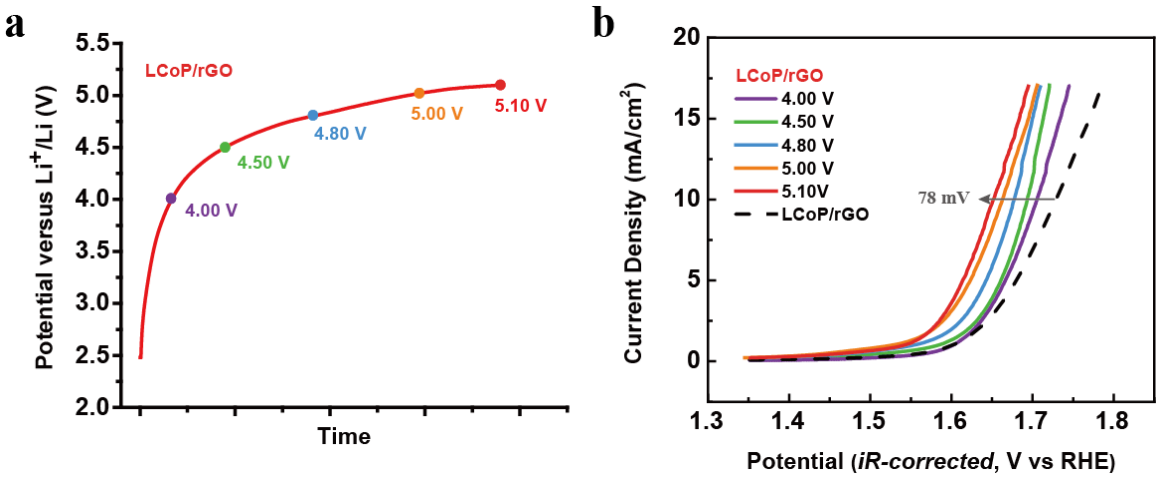

Fig. S7 (a) A typical charging curve of LCoP/rGO. (b) LSV polarization curves of LCoP/rGO charged to different potentials in 0.1 M KOH (loading = 0.5 mg/cm^2).

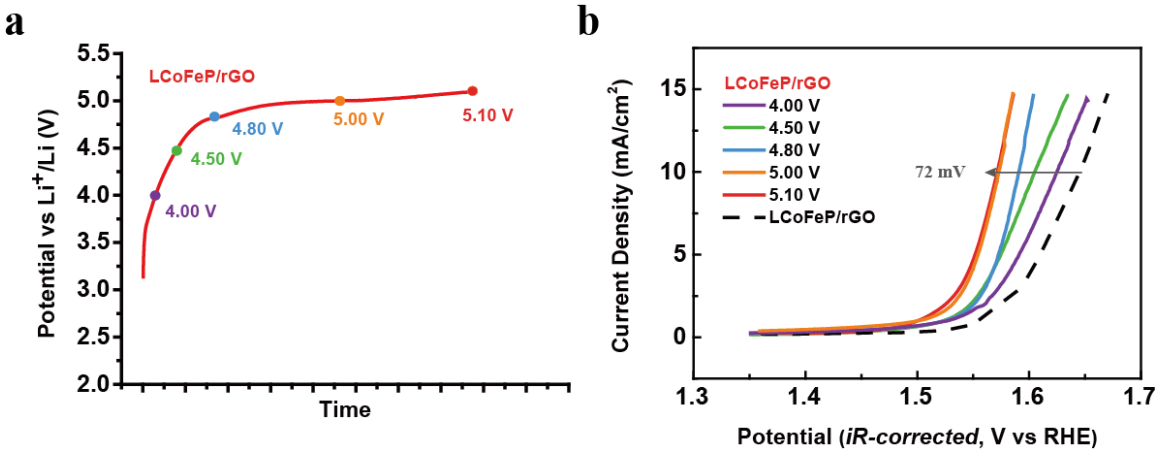

Fig. S8 (a) A typical charging curve of LCoFeP/rGO. (b) LSV polarization curves of LCoFeP/rGO charged to different potentials in 0.1 M KOH (loading = 0.5 mg/cm^2).

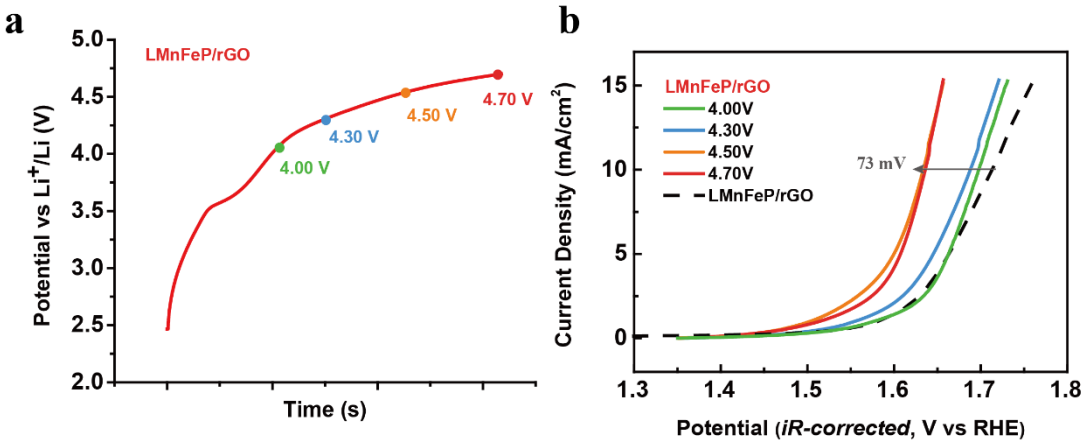

Fig. S9 (a) A typical charging curve of LMnFeP/rGO. (b) LSV polarization curves of LMnFeP/rGO charged to different potentials in 0.1 M KOH (loading = 0.5 mg/cm^2).

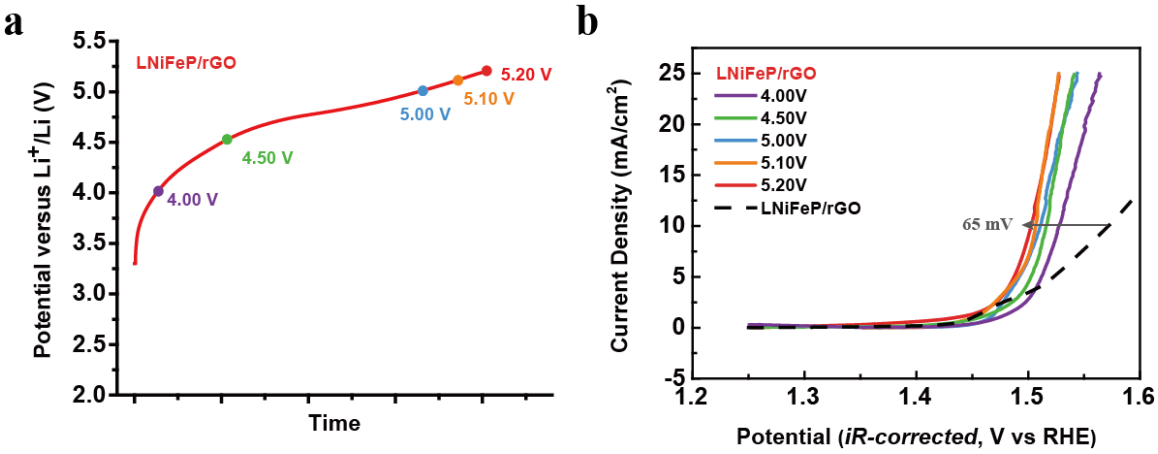

Fig. S10 (a) A typical charging curve of LNiFeP/rGO. (b) LSV polarization curves of LNiFeP/rGO charged to different potentials in 0.1 M KOH (loading = 0.5 mg/cm^2).

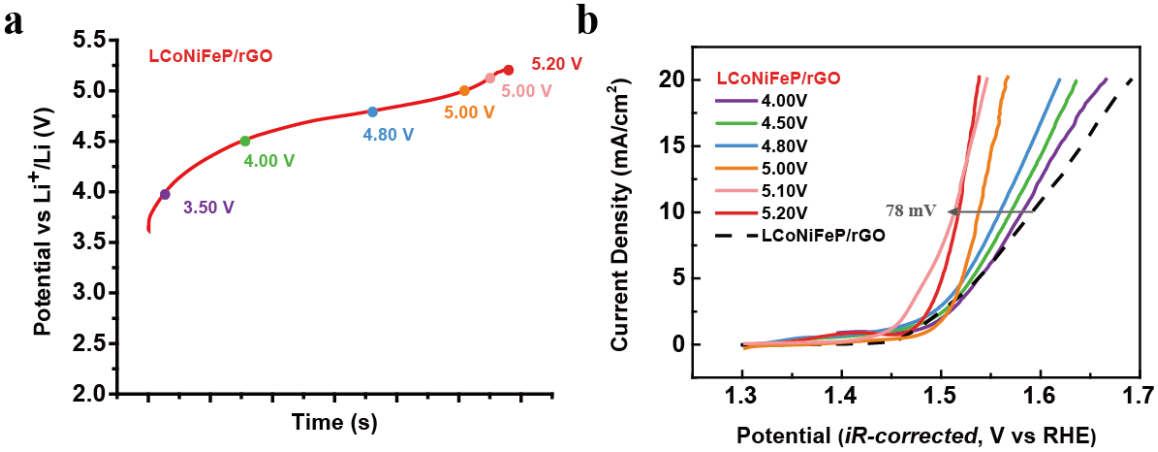

Fig. S11 (a) A typical charging curve of LCoNiFeP/rGO. (b) LSV polarization curves of LCoNiFeP/rGO charged to different potentials in 0.1 M KOH (loading = 0.5 mg/cm^2).

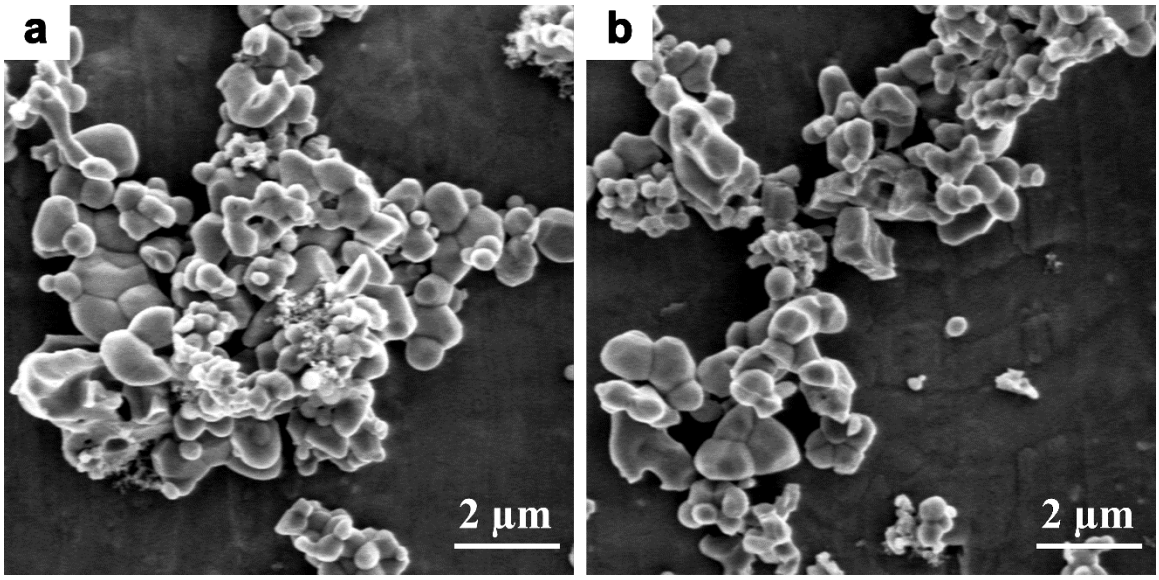

Fig. S12 SEM images of LCoP (a) before and (b) after electrochemical tuning. The small particles showed in both images was the conducting additive carbon black introduced during catalyst ink preparation.

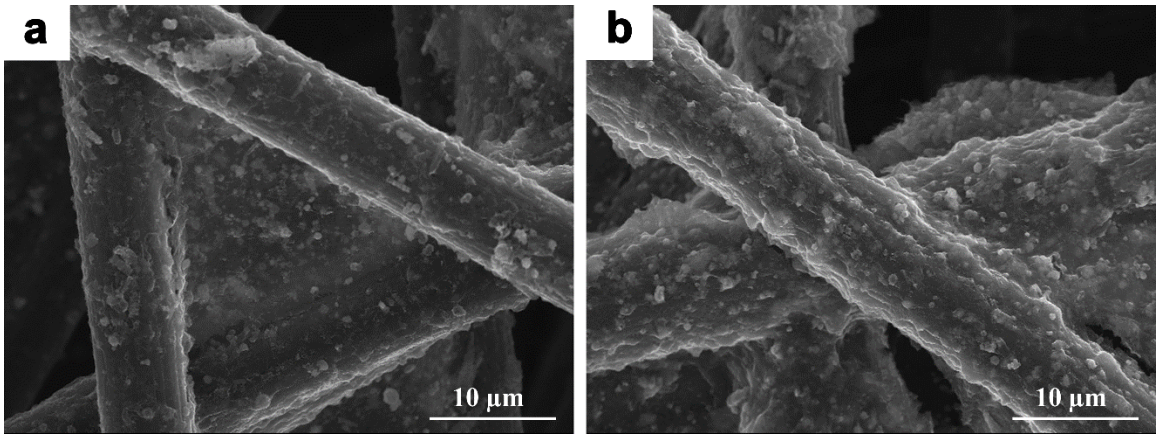

Fig. S13 SEM images of LCoP/rGO loaded on carbon fiber paper (a) before and (b) after electrochemical tuning.

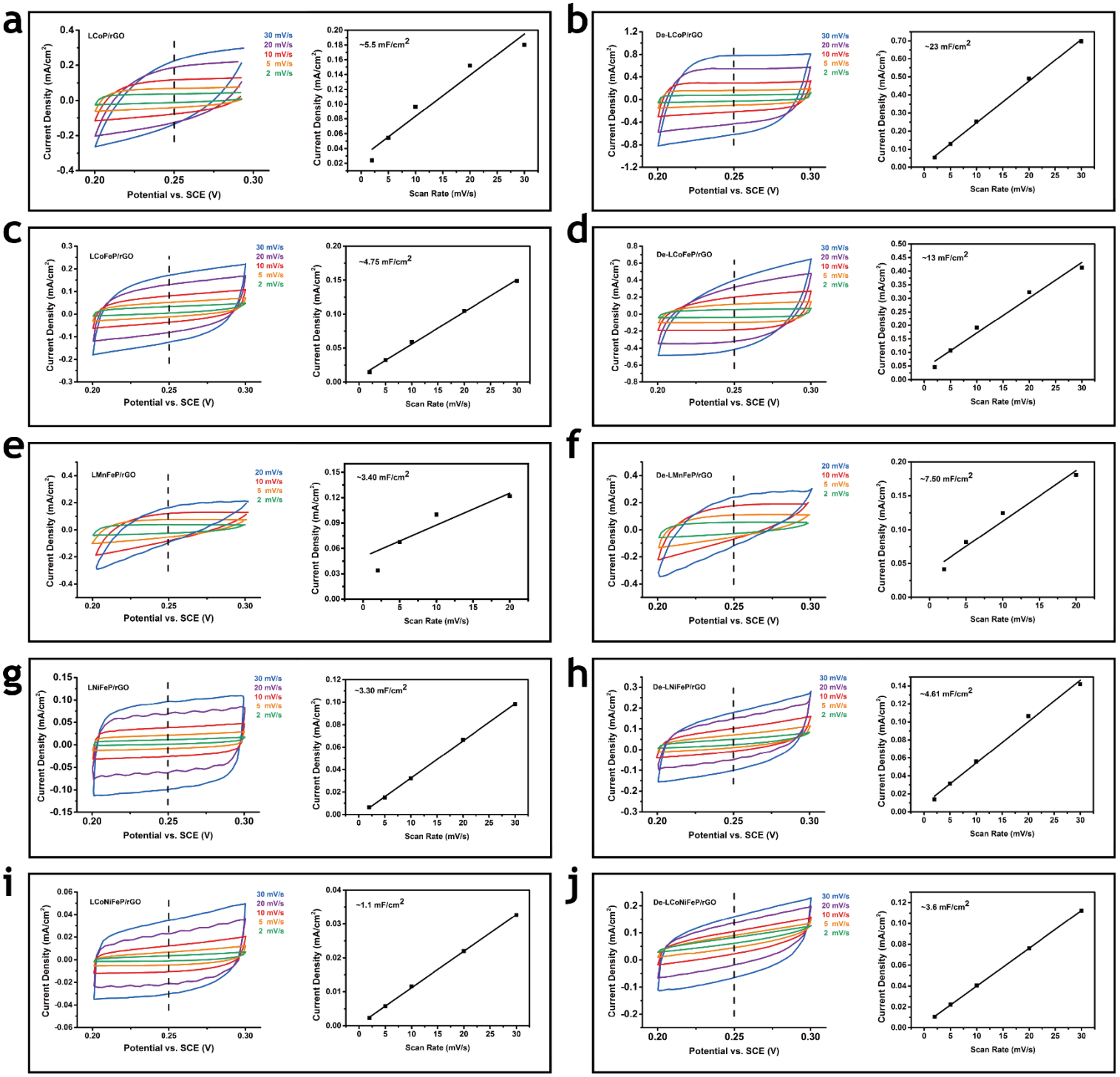

Fig. S14 EDLC curves and linear fit of current densities at 0.25 V versus scan rates of LMP/rGO and De-LMP/rGO.

Table S2 Summary of the EDLC of the catalysts before and after the electrochemical tuning.

Sample	EDLC (mF/cm^2)	Sample	EDLC (mF/cm^2)	EDLC Increase (x times)	OER Improvement (mV at 10 mA/cm^2)
LCoP	1.25	De-LCoP	11.20	9.0	126
LCoP/rGO	5.50	De- LCoP/rGO	23.00	4.2	78
LCoFeP/rGO	4.75	De-LCoFeP/rGO	13.00	2.7	72
LMnFeP/rGO	3.40	De- LMnFeP/rGO	7.50	2.2	73
LNiFeP/rGO	3.30	De- LNiFeP/rGO	4.61	1.4	65
LCoNiFeP/rGO	1.10	De- LCoNiFeP/rGO	3.60	3.3	78

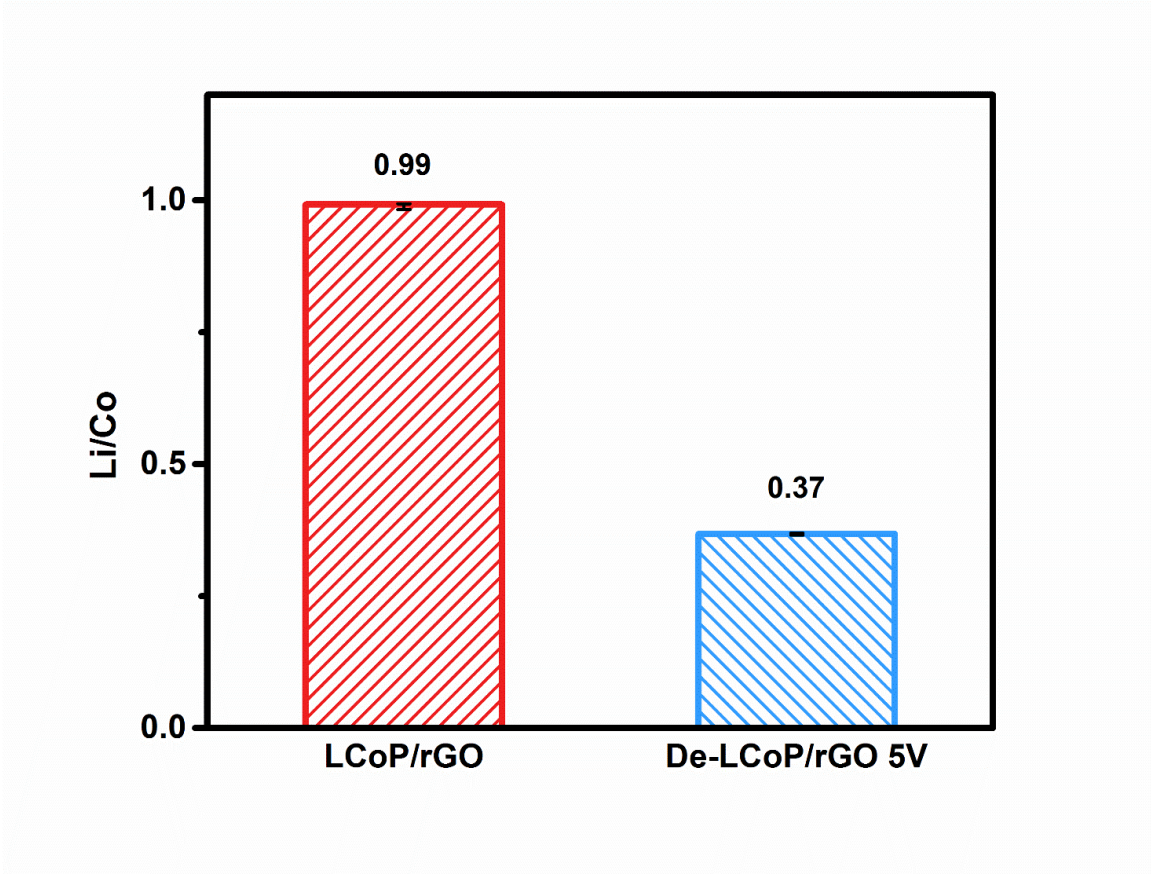

Fig. S15 Li/Co atomic ratio of LCoP/rGO and De-LCoP/rGO obtained by ICP-MS.

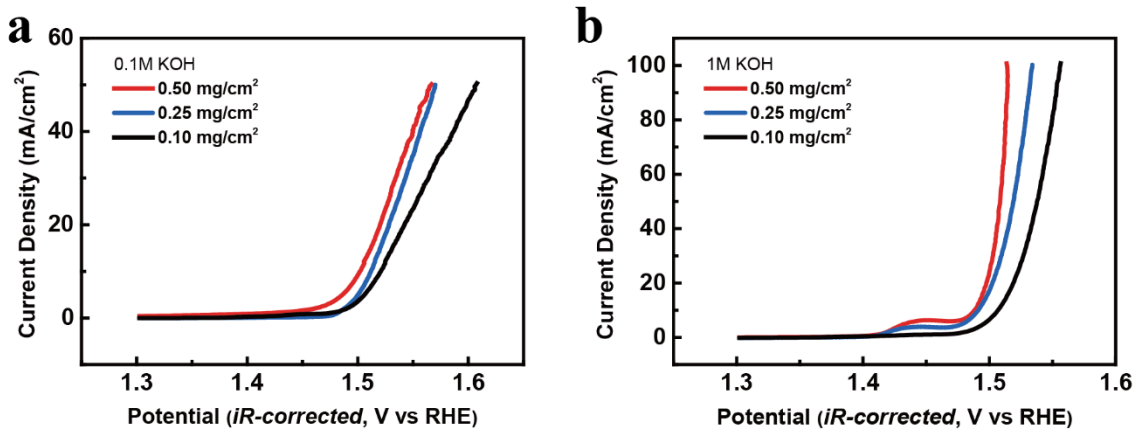

Fig. S16 LSV polarization curves of De-LNiFeP/rGO on CFP with different mass loadings in (a) 0.1 M and (b) 1M KOH.

Table S3 OER activities of some benchmark catalysts in alkaline solution

Material	Electrolyte	Mass Loading (mg/cm^2)	Current Density	Potential (V)	Tafel Slope (mV/dec)	Reference
De-LNiFeP/rGO	0.1 M KOH	0.5	10 mA/cm^2 (20 mA/mg)	1.504	57.5	This work
	0.1 M KOH	0.25	10 mA/cm^2	1.512	36.1	This work
	0.1 M KOH	0.1	10 mA/cm^2	1.521	54.6	This work
	1 M KOH	0.5	10 mA/cm^2 (20 mA/mg)	1.488	33.6	This work
	1 M KOH	0.25	10 mA/cm^2	1.491	39.0	This work
	1 M KOH	0.1	10 mA/cm^2	1.507	38.7	This work
RuO_2	0.1 M KOH	/	10 mA/mg	1.528	N.A.	8
IrO_2	0.1 M KOH	/	10 mA/mg	1.518	N.A.	8
Co_3O_4/N-rmGO	1 M KOH	1.0	10 mA/cm^2	1.540	67	13
Co_3O_4C-NA	0.1 M KOH	0.2	10 mA/cm^2	1.520	70	14
$Ni_{0.75}Co_{0.25}O_x$	1 M KOH	~0.001	10 mA/cm^2	1.575	35	10
$Mn_3O_4/CoSe_2$	0.1 M KOH	0.2	10 mA/cm^2	1.680	49	16
$Ba_{0.5}Sr_{0.5}Co_{0.8}Fe_{0.2}O_3$	0.1 M KOH	0.25	10 mA/cm^2	~1.59	48	17
NiFe-LDH/CNT	0.1 M KOH	0.25	10 mA/cm^2	1.538	35	19
De-$LiCo_{0.33}Ni_{0.33}Fe_{0.33}O_2$	0.1 M KOH	0.1	5 mA/cm^2	1.525	35	31

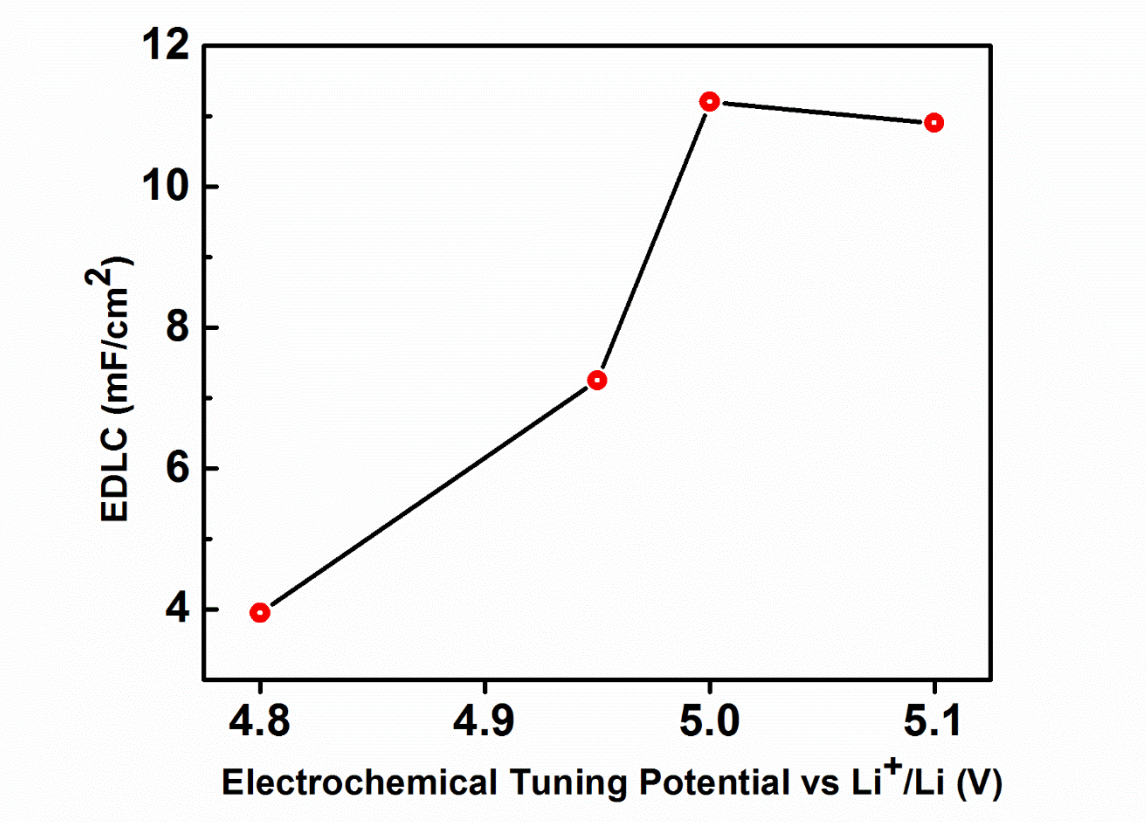

Fig. S17 The relationship between EDLC and electrochemical tuning potential for LCoP.

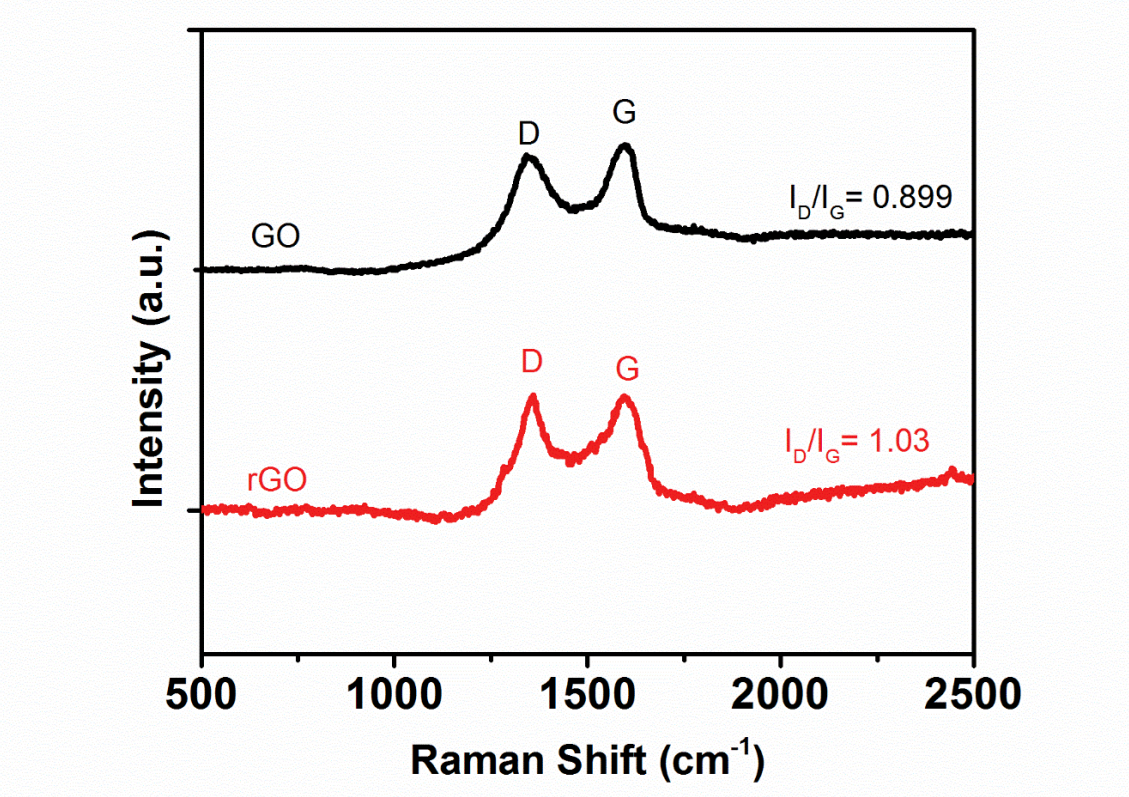

Fig. S18 Raman spectrum of GO and rGO indicating the successful reduction of GO by ascorbic acid. The ratio of D/G increased significantly, which agrees well with the Raman spectrum of the GO reduced by hydrazine.

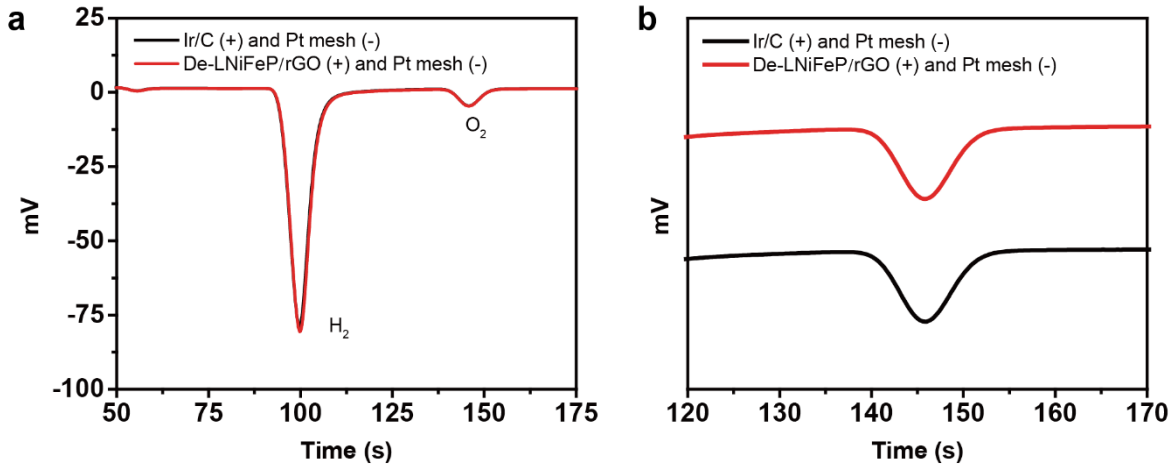

Fig. S19 (a) Gas chromatography measurements of O_2 produced by De-LNiFeP/rGO and Ir/C benchmark (counter electrode is Pt mesh). (b) Enlarged region of O_2 peaks. The catalysts were operated at 20 mA/cm^2 and the sampling was carried out using Ar flow as the carrier gas. The H_2 and O_2 peaks of the two catalysts overlap perfectly with each other, indicating the high Faradic Efficiency of the De-LNiFeP/rGO catalyst in OER.

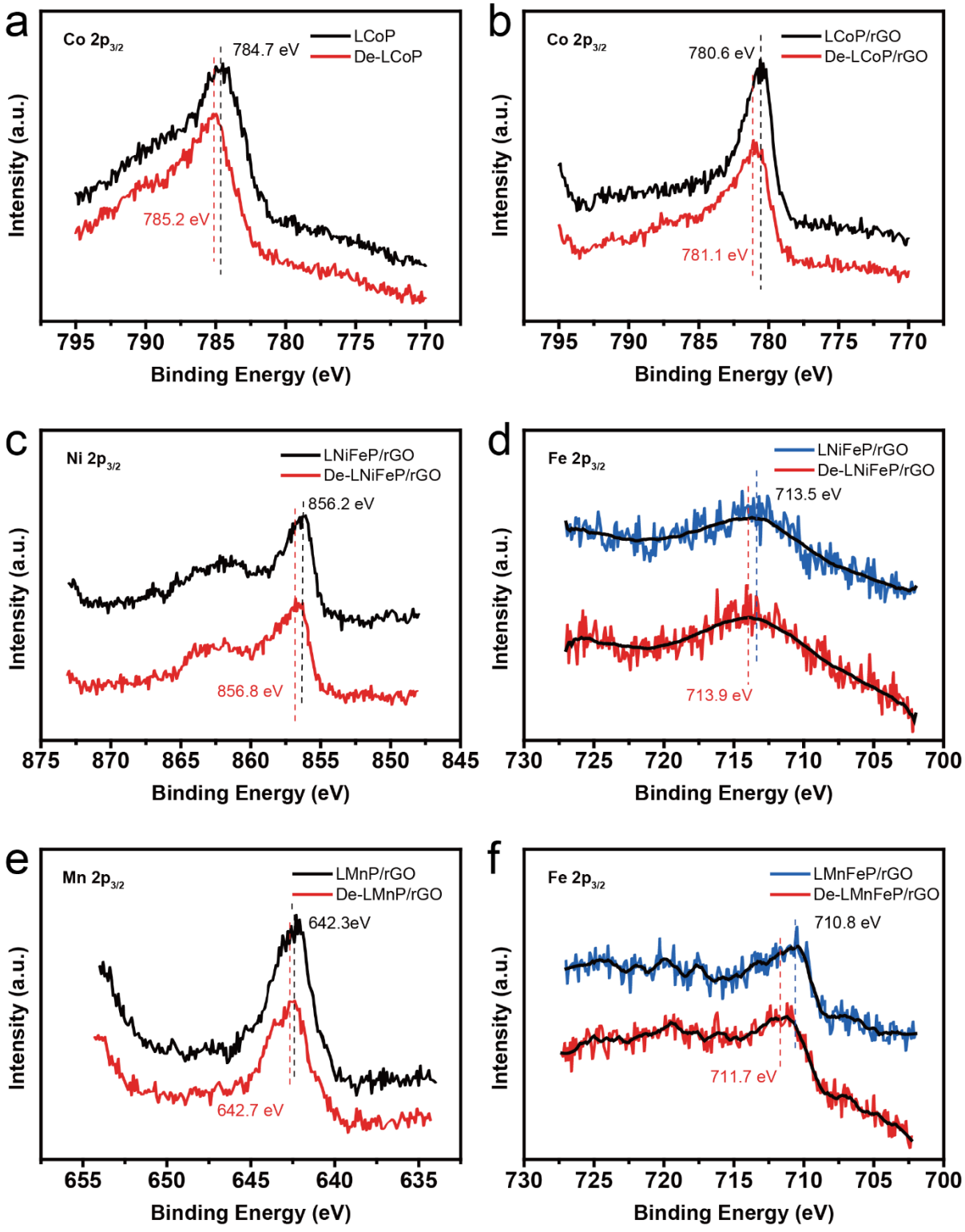

Fig. S20 XPS spectrum of (a) Co $2p_{3/2}$ peaks of bulk LCoP, (b) Co $2p_{3/2}$ peaks of LCoP/rGO, (c) Ni $2p_{3/2}$ peaks of LNiFeP/rGO, (d) Fe $2p_{3/2}$ peaks of LNiFeP/rGO, (e) Mn $2p_{3/2}$ peaks of LMnFeP/rGO and (f) Fe $2p_{3/2}$ peaks of LMnFeP/rGO before and after electrochemical tuning.